First International Conference on
Bio-based Building Materials

June 22nd - 24th 2015
Clermont-Ferrand, France

ON THE MECHANICAL CHARACTERIZATION OF A SUNFLOWER-BASED BIOCOMPOSITE USING THE GRID METHOD

S. Sun[1], E. Toussaint[1,*], M. Grédiac[1], J.-D. Mathias[2]

[1] Clermont Université, Université Blaise Pascal, Institut Pascal, UMR CNRS 6602 BP 10448, 63000 Clermont-Ferrand, France

[2] IRSTEA, Laboratoire d'Ingénierie pour les Systèmes Complexes, 9 Avenue Blaise Pascal, CS20085, 63178 Aubière, France

*Corresponding author; e-mail: evelyne.toussaint@univ-boclermont.fr

Abstract

This work is part of a project aimed at developing a new biocomposite material that can be used for building thermal insulation purposes. It deals with the mechanical characterization of this material, which is mainly made of sunflower stem chips and of biomatrix derived from chitosan, the latter being used as binder between the chips. Indeed, panels made of this material must exhibit minimum mechanical properties to be able to sustain various mechanical loads such as dead weight or local stress peaks due to mounting on walls. The goal is to investigate experimentally the link between the macroscopic response of the panels and phenomena that occur at the scale of the constituents, namely the bark and pith chips. The grid method, which is one of the full-field measurement systems employed in experimental mechanics to measure displacement and strain fields, is employed because of the very heterogeneous nature of this material. Heterogeneity is due to both the contrast in rigidity between bark and pith and to the presence of voids within the material. Because of the voids and the pith, a specific marking for the specimen surface under investigation has been developed. Compression tests performed on small briquettes made of this material provides useful information on the local response of the constituents. This also helps establishing a link with the global response of the tested briquettes. Typical experimental results will be shown and analysed during the presentation.

Keywords:

Biocomposite, biomatrix, chitosan, composite, displacement and strain measurements, grid method, sunflower

1 INTRODUCTION

This work deals with the mechanical characterization of biocomposites panels composed of sunflower stems and a biomatrix derived from chitosan. These panels are developed for building thermal insulation purposes, and must exhibit minimum mechanical properties to be able to sustain various mechanical loads such as dead weight or local stress peaks due to the wall-mounting process.

Sunflowers are agricultural by-products which are cheap and abundant. Many environmentally-friendly products are now employed in civil-engineering (see for instance [Roma 2008], [Ortiz 2009], and [Benfratello 2013]). The biocomposite studied here is very heterogeneous: it is composed of stiff bark and soft pith chips extracted from the sunflower stems on one side [Sun 2013], and of a biopolymer matrix (chitosan) which acts as binder between the chips on the other side. The bark provides the main contribution to the mechanical properties of the composite in terms of stiffness and strength. The pitch, which thermal conductivity λ=0.04 W/mK provides the main thermal insulation properties. The main objective of the present paper is to understand the link that exists between local phenomena that occur in such very heterogeneous materials and the global mechanical behaviour of the biocomposite at the macroscopic scale. For that purpose, compression tests were performed on small briquettes and a full-field measurement system was employed in order to see if a difference could be detected between the mechanical responses of the components of the sunflower stems.

The material studied is first briefly described in the first section of the paper. Then the full-field measurement technique used to measure both displacement and strain fields on the front face of the tested specimens, namely the grid method is described. The obtained results are then discussed.

2 MATERIALS, SPECIMENS AND TESTING CONDITIONS

The biocomposites were obtained by mixing bark and pith chips with a biomatrix derived from chitosan (see Fig 1). Bark and pith chips were first placed in a plastic container. The desired quantity of biomatrix was then added and mixed with the chips by hand using a stainless spatula. Sunflower stems are abundant with a world sunflower crop production that reached 24.84 millions ha in 2012. Consequently, this material does not require specific agricultural fields and is available. In addition to being abundant, sunflower stems are cheap. Chitosan is a biopolymer derived from the shells of sea crustaceans such as shrimps or crabs. It is widely commercially available and potentially cheap, depending on the quality and quantity purchased for a given application. The characteristics of the biomatrix employed here were adjusted to reach a viscosity and wettability values suitable for bark and pith chips impregnation (see [Mati-Baouche 2014]). The solvent of the biomatrix is simply water containing a low percentage of acetic acid (1%). This biomatrix is liquid before using it to impregnate the chips and becomes solid after drying.

Fig. 1: Constituents of the biocomposite.

Two mixes were considered in this study. They are defined by the mass percent fraction of chitosan that was equal to 6.25% or 4.15%. These percentages are small because of the cost of the chitosan, its environmental impact and its low insulating properties. The size of the bark and pith chips measured between 3 and 5 mm to avoid to being too small or too large. The obtained mixes were placed in a small mold which dimensions are 50x92x180 mm^3. A compaction pressure of 32 kPa was applied. After drying, briquettes were obtained. They were cut with a saw band to obtain the desired size of the specimens: about 50x80x122 mm^3. Typical results obtained with two specimens by mixture are given and discussed in this study. The biocomposite under study features numerous voids, which are clearly visible to the naked eye and cannot be considered as defects if their volume fraction remains low. The thermal conductivity measured with the hot-wire method is equal to about λ=0.06 W/mK.

The specimens were subjected to compression tests performed using a ± 20 kN Zwick-Roell testing machine. The tests were displacement-controlled with a cross-head speed equal to 0.02 mm/s, the maximum imposed displacement on the upper side of the specimens being equal to 4 mm.

Heterogeneous stress and strain fields were expected to occur in these specimens because of the very heterogeneous nature of this type of composite material. A full-field measurement method was therefore employed to detect and quantify these heterogeneities. The grid method (see [Grediac 2013]) was recently successfully employed in situations for which high strain gradients were measured thanks to a good compromise between spatial resolution in strain maps (defined here by the shortest distance between two spatially independent measurements) and strain resolution of this technique (defined here by the change in quantity being measured that causes a change in the corresponding indication greater than one standard deviation of the measurement noise [Chrysochoos 2012]). A specific technique for marking the surface has been developed because of the softness of the material under study. It is presented in the following section after some recals about the principle of the so-called grid method.

3 GRID METHOD AND SURFACE PREPARATION

3.1 Principle

The grid method consists first in transferring a grid on the surface under investigation. The idea is then to capture images of this grid with a camera and to extract displacement and strain fields from the grid images while the specimen under test deforms. It can be shown that the displacement and strain fields can be deduced from the images using a processing technique based on Fourier transform [Surrel 2000]. These images are processed after testing using a specific grid image processing procedure which relies on the calculation of the phase of this pseudo-periodic surface marking when displacement is the sought quantity. Indeed displacements are directly proportional to phase changes between the two grids. The phase derivatives variations are considered when strain components are to be determined. It is to note that a recent procedure that is aimed at removing a significant part of the negative effects of the printing defects on strain fields has been employed in the current study [Badulescu 2011]. With this technique, the resolution in displacement is typically equal to some micrometers and the resolution in strain to some hundreds of microstrains, depending on lighting and on the quality of the grid and the camera.

3.2 Surface preparation

Voids visible on the front face of the specimens were filled using sealant (Sikaflex-11FC+, Le Bourget, France) to limit disturbance in the measurement close to these zones which would be due to the lack of marking. The sealant is a one-component polyurethane that has a pasty texture before applying it on the specimen, and remains pasty after drying. The Young's modulus of this material is very low: E=0.6 MPa after drying and its deformation at failure is equal to 700%. The Young's modulus of the pith is approximately equal to 0.7 MPa but it is impregnated with the bio-matrix, whose Young's modulus is equal to 4 MPa. Consequently, one can reasonably assume that the impact of this filling material on the response

of the specimen is negligible. It has been confirmed by the fact that the Young's modulus of the composite measured hereafter is the same as that measures on specimens without sealant.

After filling the voids with sealant, the surface was carefully sanded and cleaned. The grid was directly painted onto the surface using a stencil. This allows avoiding the transfer of a grid and then the use of a layer of adhesive that would modify the rigidity of the specimen. White paint was first spayed on the surface of the specimen. The stencil was then placed on this surface and a black acrylic ink was spayed though the stencil with a V type Paasche airbrisher. The minimum size of the square holes was equal to 0.4 mm. This finally leads to a grid featuring a frequency of 1.25 lines/mm, thus a nominal pitch is equal to 0.8 mm. Figure 2 shows the grid obtained after painting.

a- raw surface after cutting

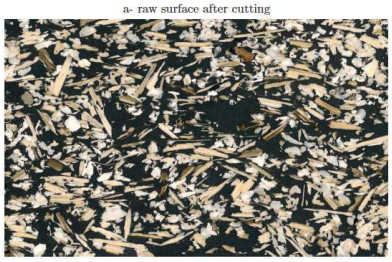

b- front face after filling with sealant and sanding

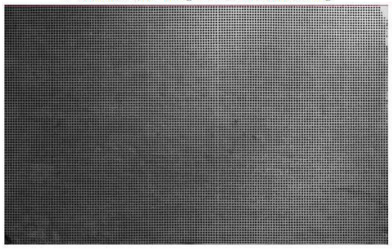

c- grid painted on the front face of the specimen after filling with sealant and sanding

Fig. 2: Front face of a specimen

3.3 Metrological performance of the measuring technique

The grid pitch given above enables us to estimate the spatial resolution of the measuring technique. The spatial resolution can be estimated as being equal to 6 times the standard deviation σ of the Gaussian envelope used in the windowed Fourier transform (WFT). Here σ □□□equal to 9 pixels since the grid is encoded with 9 pixels. The spatial resolution is thus equal to 0.8x6=4.8 mm or 9X6=54 pixels. This means that an independent value is found every 4.8 mm or 54 pixels in the image, even though a difference value for displacement or strain is displayed at every pixel.

3.4 Image acquisition

A SENSICAM QE camera featuring a 12-bit/1040x1376 pixels sensor was used to capture the images of the grid. The maximum size of the field that can be investigated was about 92x122 mm^2. The optical magnification was adjusted as well as the perpendicularity of the observation axis thanks to a mounting plate on which the camera was fixed. The grid was illuminated by three flexible and movable light guides fed by a KL 2500 LCD cold light source.

4 RESULTS

4.1 Global response

An example of mean strain ε_{yy}^{mean}/mean stress σ_{yy}^{mean} curve is presented in Fig.3, where y is the vertical axis and x is the horizontal one. Comparing the mean strain measured from full-field measurement and that deduced from the displacement of the moving grip provided by the testing machine shows that the former is lower. It is a consequence of clearance take-up that occurs during the first stage of the test. All the curves shown in the following figures were obtained with full-field measurement to avoid the influence of the clearance take-up. Curves in Fig. 3 are non-linear, which illustrates a progressive apparent softening of the material. It is interpreted below as an effect of damage.

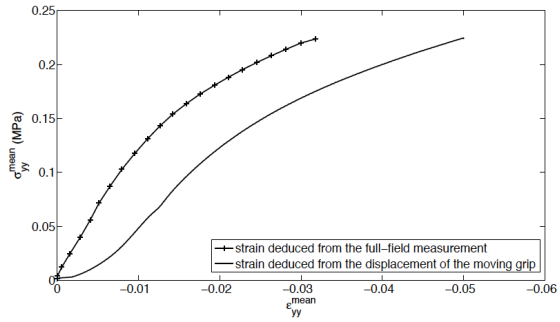

Fig. 3: σ_{yy}^{mean} vs ε_{yy}^{mean}

A residual strain appeared after unloading. It is visible in Fig. 4 were ε_{yy}^{mean} vs. the number of the image is shown. ε_{yy}^{mean} increases in a fairly linear rate which is a consequence of the fact that the test is displacement-controlled. A residual strain equal to about 0.5% can be seen at the end of the test. It is due to irreversible degradation of the material during the test.

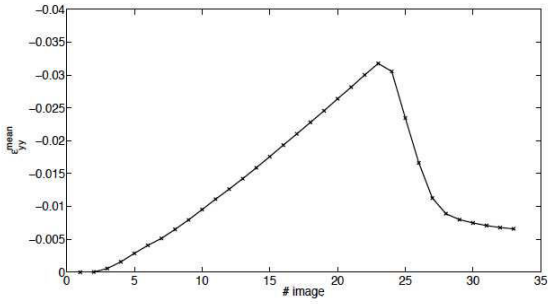

b- ϵ_{yy} vs. image #

Fig. 4: Global response ε_{yy}^{mean}

Figure 5 shows the curves obtained for the four specimens during their first loading. The influence of the mass percent fraction of chitosan is visible. Beyond the first phase of the response, both specimen prepared with a 6.25% mass percent fraction of chitosan are stiffer than those prepared with a 4.15% mass percent fraction of chitosan. This result is confirmed by the apparent secant modulus deduced from the curves avec a [0-3] % interval which are reported in Table 1: they are greater for specimens prepared with a 6.25% mass percent fraction of chitosan.

Tab. 1: Apparent secant modulus.

Specimen	6.25% (1)	6.25% (2)	4.15% (1)	4.15%(2)
E(MPa)	7.60	5.90	5.25	5.42

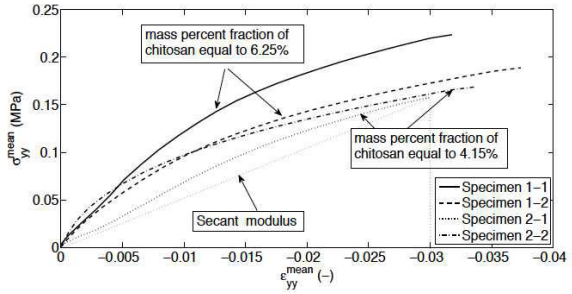

Fig. 5: Global response ε_{yy}^{mean}

4.2 Local response

The next step was to observe the underlying mechanisms that occur as the load increase, and to establish the link between local and global response. Fig. 6 shows the relative vertical displacement field at maximum imposed displacement for a specimen with 6.25% mass percent fraction of chitosan. All dimensions are given in pixels. This map is obtained by subtracting at each pixel the measured displacement and the mean value of the displacement field.

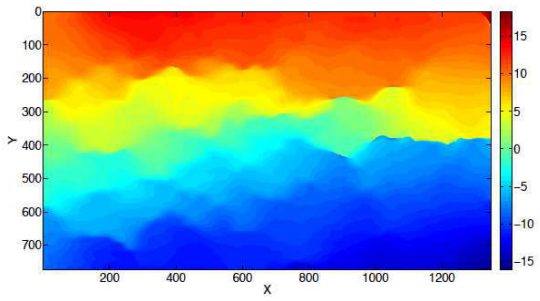

Fig. 6: Relative vertical displacement

It is quite logical to see that the displacement increases from the bottom to the top of the specimen, since a compression test is performed (the moving grip is located at the top). The corresponding strain field ε_{yy} is shown in Fig. 7. It is plotted using a logarithmic scale.

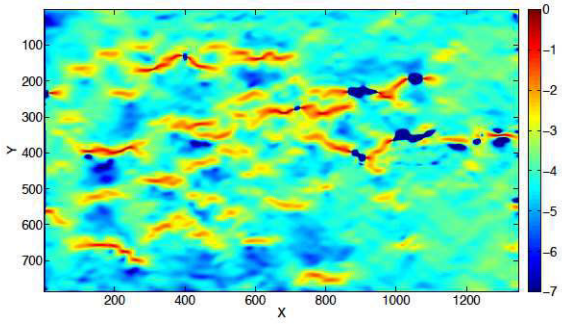

Fig. 7: Strain field at maximum. Logarithmic scale.

The strain distribution features very localized peaks. They correspond to situations for which sealant and thus the grid are pushed aside as voids collapse. This means that the strain values measured at these points are very high, but probably flawed because of the local out-of-plane movement of the sealant.

4.3 Comparison between local and global responses

Local strain value ε_{yy} at any pixel are compared to the mean strain ε_{yy}^{mean}. This is done by calculating the ration r_y defined by $r_y = \frac{\varepsilon_{yy}}{\varepsilon_{yy}^{mean}}$

The corresponding map, superimposed to the fraont face of the specimen is presented in Fig. 8. The ratio is mainly lower than 1, but features very localized peaks which are muck greater than 1. Peaks are mainly localized in the voids filled with sealant.

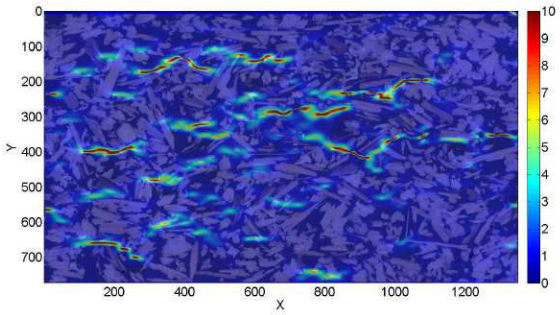

Fig. 8: Superimposition of the r_y map on the front face of the specimen.

4.4 Comparison between the behavior of bark and pith

As the stiffness of each constituent of the bio-composite is very different, the strain distribution of both bark and pith is studied. For that purpose, three masks, corresponding to, the zone covered by sealant, bark and pith, respectively are obtained by thresholding the gray levels in the images, first for the sealant, then for the bark and the pith using a trial-and-error procedure. The strain field in the pitch and bark are presented in Fig. 9.

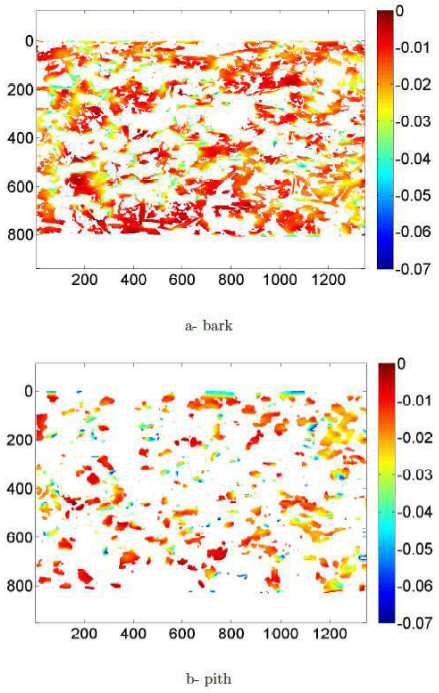

Fig. 9: Strain field in bark and pith at maximum load.

No clear difference can be observed at this stage to the naked eye. Considering now the mean strain over these zones enables us to see the difference in behavior between the bark and the pith. This is illustrated in Fig. 10.

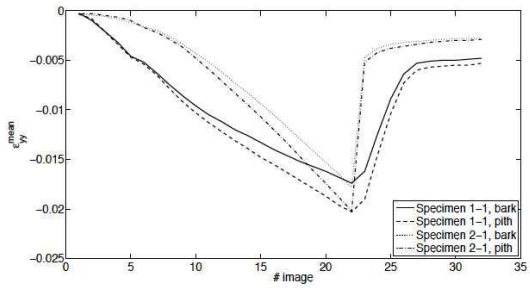

Fig. 10: Mean strain in bark and pith vs. # image, specimens 1-1 and 2-1 (6.25% and 4.15% mass percent fraction of chitosan).

It can be observed that the pith sustains a greater strain than the bark in both cases, and that this difference increases during the loading phase. This result seems logical since pith is softer than bark. This is certainly also due to the very non-linear response of pith compared to bark, since the stress-strain curve of the former exhibits a significant plastic zone.

5 CONCLUSION

The mechanical behavior of a sunflower/chitosan biocomposite was studied in this paper. Strain maps have two levels of heterogeneities. First, it was shown that the mechanical response was mainly governed by void crushing, which is equivalent to very high local strain. Second, it was shown that the strain level was greater in pith than in bark, which is due to the difference in stiffness between these two phases. The influence of the percentage of chitosan was also clearly observed.

6 ACKNOWLEDGEMENTS

The authors would like to thank the French National Research Agency (ANR), Céréales Vallée, and ViaMéca for their financial support (ANR-10-ECOT-004 Grant).

7 REFERENCES

[Roma 2008], Roma, L.C., Martello, L.S. and Savastano, H. Evaluation of mechanical, physical and thermal performance of cement-based tiles reinforced with vegetable fibers, Construction and building materials, 2008, 22(1), 668-674.

[Ortiz 2009], Ortiz, O., Castells, F. and Sonnemann, G. Sustainability in the construction industry: A review of recent developments based on lca. Construction and Building Materials, 2009, 23(1):28-39.

[Benfratello 2013], Benfratello, S., Capitano, C. Peri, G., Rizzo, G., Scaccianoce, G. and Sorrentino, G., Thermal and structural properties of a hemp-lime biocomposite, Construction and Building Materials 2013, 48:745--754.

[Sun 2013], Sun, S., Mathias, J.-D., Toussaint, E. and Grédiac, M., Hygromechanical characterization of sunfower stems, Industrial Crops and Products, 2013., 46:50—59.

[Mati-Baouche 2014], Mati-Baouche, N. De Baynast, H., Sun, S., Lebert, A., Sacristan Lopez-Mingo, C.J., Leclaire, P. and and Michaud, P., Mechanical, thermal and acoustical characterizations of a insulating bio-based composite made from sunflower stalks particles and chitosan., Industrial Crops and Products, 2014, 58: 244-50

[Grediac 2013], Grédiac and Toussaint, E., Studying the Mechanical Behaviour of Asphalt Mixture with the Grid Method, Strain, 2013, 49: 1-15

[Chrysochoos 2012], Chrysochoos, A. and Surrel, Y., Chapter1. Basics of metrology and introduction to techniques, In M. Grédiac and F. Hild, editors, Full-field measurements and identification in solid mechanics, pages 1-29, Wiley, 2012.

[Surrel 2000], Surrel, Y., Photomechanics, Topics in Applied Physic 77, chapter Fringe Analysis, pages 55—102, Springer, 2000.

[Badulescu 2011], Badulescu, C., Greédiac, M., Haddadi, H., Mathias, J.-D., Balandraud, X. and Tran, H.-S., Applying the grid method and infrared thermography to investigate plastic deformation in aluminium multicrystal. Mech. Mater. 2011, 43, 36–53.